

The Super-Kamiokande Experiment *

Christopher W. Walter[†]

Department of Physics, Duke University,
Durham, NC 27708 USA
chris.walter@duke.edu

Super-Kamiokande is a 50 kiloton water Cherenkov detector located at the Kamioka Observatory of the Institute for Cosmic Ray Research, University of Tokyo. It was designed to study neutrino oscillations and carry out searches for the decay of the nucleon. The Super-Kamiokande experiment began in 1996 and in the ensuing decade of running has produced extremely important results in the fields of atmospheric and solar neutrino oscillations, along with setting stringent limits on the decay of the nucleon and the existence of dark matter and astrophysical sources of neutrinos. Perhaps most crucially, Super-Kamiokande for the first time definitively showed that neutrinos have mass and undergo flavor oscillations. This chapter will summarize the published scientific output of the experiment with a particular emphasis on the atmospheric neutrino results.

I. INTRODUCTION AND PHYSICS GOALS

The Super-K collaboration is the combination of two previous successful collaborations. The first was the Kamiokande [1, 2] experiment which was located in the same mine as Super-K and had a fiducial mass approximately 20 times smaller than Super-K. The second was the IMB experiment [3, 4] which was located in the Morton Salt mine in Ohio. Grand Unified models such as SU(5) [5] predicted that the proton would decay at a rate visible by modest size detectors and both of these experiments were originally built to search nucleon decay into the mode favored by SU(5) which is $p \rightarrow e^+ \pi^0$.

Although neither of these experiments observed the decay of the proton, they did measure a statistically significant anomaly in the expected background to the proton decay search from neutrino interactions on the water in the tanks. One explanation for this effect was that some of the neutrinos were oscillating into an un-observable flavor and thus giving less background than expected. At the same time two detectors made of iron the NUSEX [6] and Frejus [7] experiments saw a result which was consistent with the expectation but with much lower statistics. Super-Kamiokande was designed to definitively determine whether or not oscillations were indeed taking place.

Additionally, by scaling up the size from previous detectors, Super-Kamiokande offered new hope to finally observe the decay of the nucleon and also to try to answer the crucial question of whether neutrinos produced in the nuclear burning in the sun oscillated into non-detectable flavors on their way to the earth. Previous generations of experiments had not seen as many neutrinos from the sun as predicted by solar models. With a large mass, good energy resolution, and the ability to point neutrinos

back to the sun in real-time, Super-Kamiokande was designed first of all to confirm the effect with high statistics and then to determine what the parameters of oscillation were.

II. THE SUPER-KAMIOKANDE DETECTOR

Super-Kamiokande is a 50 kiloton water Cherenkov detector located at the Kamioka Observatory of the Institute for Cosmic Ray Research, University of Tokyo. Figure 1 shows a diagram of the Super-Kamiokande detector. The detector is in the Mozumi mine of the Kamioka Mining Company in Gifu prefecture, in the Japanese alps. Super-K consists of two concentric, optically separated water Cherenkov detectors contained in a stainless steel tank 42 meters high and 39.3 meters in diameter, holding a total mass of 50,000 tons of water. The inner detector is comprised of 11,146 Hamamatsu R3600 50 cm diameter photomultiplier tubes, viewing a cylindrical volume of pure water 16.9 m in radius and 36.2 m high.

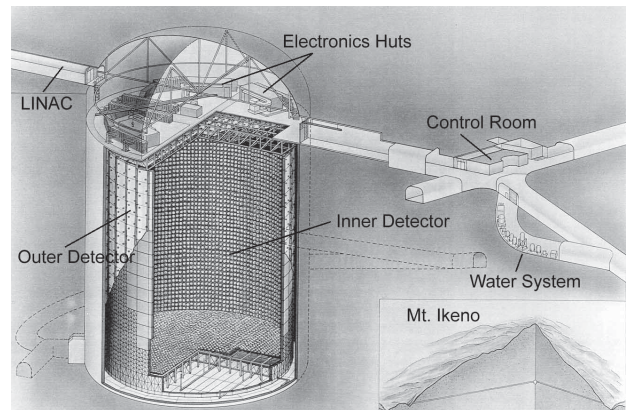


FIG. 1: An overview of the Super-Kamiokande detector site, under Mt. Ikeno from Ref. [8]. The cutaway shows the inside lined with photomultiplier tubes comprising a photo-cathode coverage of about 40%.

*Prepared for *Neutrino Oscillations: Present Status and Future Plans*, J. Thomas and P. Vahle editors, World Scientific Publishing Company, 2008.

[†]For the Super-Kamiokande collaboration.

As described more fully in Ref. [8], the detector is calibrated in energy at the 2% level over energies ranging from the MeV to the tens of GeV range. This careful calibration is key to the successful extraction of physics. It relies both on natural calibration sources such as the expected energy deposit of muons created by the cosmic rays and the decay of neutral pions produced by neutrino interactions inside the Super-Kamiokande tank, and on artificial sources including lasers, a Xenon light source, a linear accelerator [9] and a ^{16}N source [10]. Low energy radioactive background were also carefully studied, a description of the measurement of radon concentrations at Super-Kamiokande is given in Ref. [11].

Data from the detector is first collected by an on-line data acquisition system and then, after a calibration step, passed into several streams of reduction for the various analyses. Selection steps are performed to remove the background from non-neutrino induced interactions. For example, the outer detector region is used as a veto to reject cosmic-ray muons. Using the time and charge information at each photo-tube, reconstruction algorithms are applied to the data to determine a vertex for the Cherenkov light and any rings associated with the particles of the interaction. Additional likelihood-based algorithms are used to determine the properties of the particles that generated the light including their type, momenta and directions. These reconstructed physics quantities are then used for analysis. More detail about the acquisition and analysis reconstruction techniques can be found in Refs. [8, 12] and [13].

The Super-Kamiokande running periods are divided into three parts. The first, SK-I ran from 1996 to 2001. In November of 2001 an accident destroyed much of the photo-tubes of Super-K and, after a year of rebuilding the detector with half of the previous photo-tube density, SK-II ran for approximately 800 days. In June of 2006 after restoring Super-Kamiokande to its full photo-tube density a period of running known as SK-III began. During the SK-I and SK-II running period Super-Kamiokande acted as the target for the long-baseline K2K experiment. Starting in 2009, Super-Kamiokande will once again be the target of an accelerator produced neutrino beam when the T2K experiment begins.

III. PUBLISHED RESULTS FROM SUPER-KAMIOKANDE

The published scientific output of the Super-Kamiokande experiment can be roughly divided into four main categories:

1. Studies of atmospheric neutrino oscillations
2. Studies of solar neutrino oscillations
3. Searches for the decay of the nucleon
4. Searches for astrophysical sources of neutrinos

In the sections that follow, papers from all of these subjects will be reviewed. Particular attention will be paid to the history of the published papers in the atmospheric neutrino analysis.

A. Atmospheric Neutrino Oscillations

The sub-GeV R ratio [14]

In the previous results from the IMB and Kamiokande experiment it was observed that the flavor ratio of neutrinos below 1 GeV did not agree with expectation. If one took the results at face value, either there were more electron neutrinos than expected, or too few muon neutrinos. In order to study the question experimentally a measurement was made of:

$$R \equiv (\mu/e)_{DATA}/(\mu/e)_{MC}, \quad (1)$$

which served to cancel uncertainties in neutrino flux and cross-sections. In Eqn. 1, (μ/e) means the ratio of the number of measured neutrino interactions which are inferred to have come from electron and muon neutrinos respectively. The ratio is calculated separately for the reconstructed data and MC. If there is perfect agreement between data and expectation the expected value of R is one. In Super-Kamiokande, the measured value of R was:

$$R = 0.61 \pm 0.03(stat.) \pm 0.05(sys.). \quad (2)$$

This was a statistically significant result and the collaboration concluded in Ref. [14]:

“The first measurements of atmospheric neutrinos in the Super-Kamiokande experiment have confirmed the existence of a smaller atmospheric ν_μ/ν_e ratio than predicted. We obtained $R = 0.61 \pm 0.03(stat.) \pm 0.05(sys.)$ for events in the sub-GeV range. The Super-Kamiokande detector has much greater fiducial mass and sensitivity than prior experiments. Given the relative certainty in this result, statistical fluctuations can no longer explain the deviation of R from unity.”

The multi-GeV R ratio [15]

The previous result relied on events which had visible energy less than 1.33 GeV deposited in the Super-K tank (so called sub-GeV events). Although less numerous, multi-GeV events were also expected to oscillate and had the extra advantage that at high-energy the outgoing lepton direction closely followed the incoming neutrino direction. Since the neutrino oscillation probability is a function of both the distance traveled and the energy, knowing the direction of the incoming neutrino allowed the separation of neutrinos into bins of angular zenith. Based on the results of the previous experiments it was expected that neutrinos of a few GeV would need to travel thousands of kilometers before they oscillated.

Also, if muon neutrino were oscillating into tau neutrinos, the vast majority of them would not have the energy necessary to interact and produce a tau lepton. In this case, the expectation was that there would be a deficit of muon interactions coming from below.

From the data analyzed, the R ratio for the multi-GeV events was reported in Ref. [15] to be:

$$R = 0.66 \pm 0.06(stat.) \pm 0.08(sys.). \quad (3)$$

confirming the result seen in the sub-GeV sample. Crucially, the expected zenith suppression was also seen.

Evidence for oscillations [16]

In 1998, the paper ‘‘Evidence for oscillation of atmospheric neutrinos’’ was published[16]. In this paper, 535 days of data were analyzed and subdivided into sub-GeV and multi-GeV e-like and mu-like events. In this data set, a strong suppression of upward going event from muon-neutrino interactions was observed. This was quantified in terms of an asymmetry defined as $A = (U - D)/(U + D)$ where U is the number of upward-going events ($-1 < \cos \Theta < -0.2$) and D is the number of downward-going events ($0.2 < \cos \Theta < 1$). Due to the isotropic nature of the cosmic rays this asymmetry is expected to be close to zero. For the electron-neutrino sample this was found to be the case. For the muon-like events the asymmetry was found to be:

$$A = \frac{(U - D)}{(U + D)} = -0.296 \pm 0.048(stat.) \pm 0.01(sys.) \quad (4)$$

which deviates from zero by more than 6 standard deviations. Figure 2 taken from Ref. [16] shows this asymmetry as a function of momentum for both the e-like and mu-like samples. The deficit of high energy upward-going mu-like events is clearly seen.

A fit was performed over the oscillation parameter space to the $\nu_\mu \leftrightarrow \nu_\tau$ oscillation hypothesis. There were eight systematic uncertainty terms that were allowed to vary within their known ranges. Fits were also performed to the $\nu_\mu \leftrightarrow \nu_e$ hypothesis but the data did not fit this hypothesis well. The data-samples and the results of the fit are shown in the Fig. 3 also from Ref. [16].

This analysis resulted in the first allowed region for atmospheric neutrino oscillations from Super-Kamiokande, resulting in a somewhat lower allowed region than was previously obtained from the Kamiokande collaboration. In this paper the conclusion was:

Both the zenith angle distribution of μ -like events and the value of R observed in this experiment significantly differ from the best predictions in the absence of neutrino oscillations. While uncertainties in the flux prediction, cross sections, and experimental biases are ruled out as explanations of the observations, the present data are in good agreement with two-flavor $\nu_\mu \leftrightarrow \nu_\tau$ oscillations with $\sin^2 2\theta > 0.82$ and $5 \times 10^{-4} < \Delta m^2 < 6 \times 10^{-3} \text{ eV}^2$

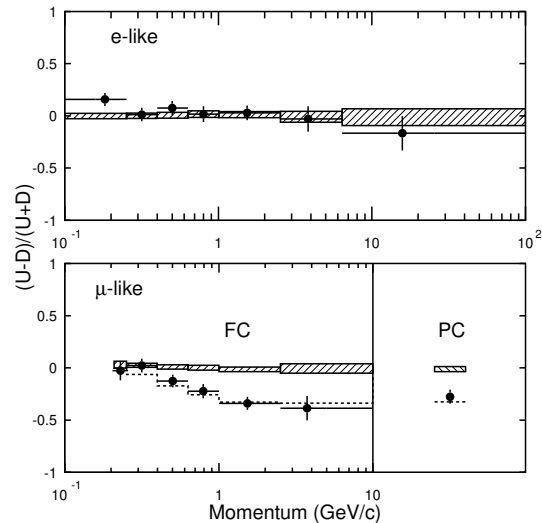


FIG. 2: The $(U - D)/(U + D)$ asymmetry as a function of momentum for FC e -like and μ -like events and PC events. While it is not possible to assign a momentum to a PC event, the PC sample is estimated to have a mean neutrino energy of 15 GeV. The Monte Carlo expectation without neutrino oscillations is shown in the hatched region with statistical and systematic errors added in quadrature. The dashed line for μ -like is the expectation for $\nu_\mu \leftrightarrow \nu_\tau$ oscillations with ($\sin^2 2\theta = 1.0$, $\Delta m^2 = 2.2 \times 10^{-3} \text{ eV}^2$). Figure and caption from Ref. [16].

at 90% confidence level. We conclude that the present data give evidence for neutrino oscillations.

It should be noted that the allowed region found in 1998 is consistent with all of the later more refined analysis, which have also all been consistent with each other.

Upward-going [17] and stopping [18] muon samples

Also analyzed separately in Refs [17] and [18] were upward through-going and stopping muon samples. Muons are created by neutrino interactions under the Super-K tank and then travel upwards, either passing through or stopping inside the detector. The through-going events were of a higher energy than the events analyzed in Ref. [16] which were completely contained inside the Super-K tank, and the stopping events were of comparable energy to the events previously considered in which the produced muon escaped the tank. The reduction process for these events was somewhat more involved since it was more difficult to remove backgrounds from entering downward-going muons.

In these two papers, the two sub-samples were fit to the oscillation hypothesis as was their ratio as a function of zenith angle. It was found that they also gave results

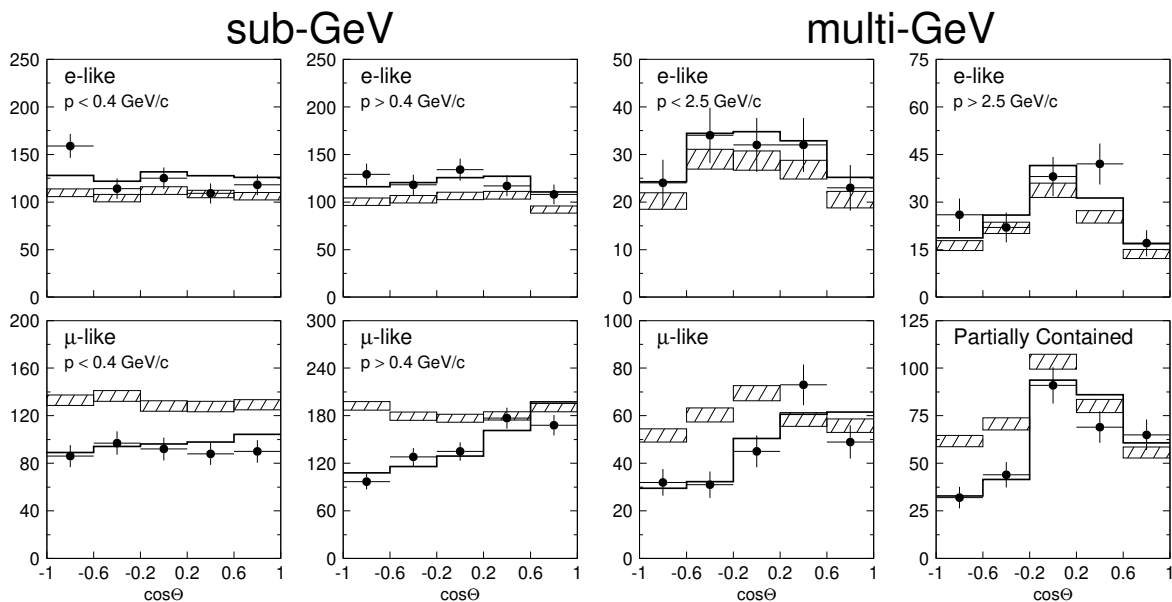


FIG. 3: Zenith angle distributions of μ -like and e -like events for sub-GeV and multi-GeV data sets. Upward-going particles have $\cos \Theta < 0$ and downward-going particles have $\cos \Theta > 0$. Sub-GeV data are shown separately for $p < 400$ MeV/ c and $p > 400$ MeV/ c . Multi-GeV e -like distributions are shown for $p < 2.5$ GeV/ c and $p > 2.5$ GeV/ c and the multi-GeV μ -like are shown separately for FC and PC events. The hatched region shows the Monte Carlo expectation for no oscillations normalized to the data live-time with statistical errors. The bold line is the best-fit expectation for $\nu_\mu \leftrightarrow \nu_\tau$ oscillations with the overall flux normalization fitted as a free parameter. Figure and caption from Ref. [16].

consistent with neutrino oscillations as presented in Ref. [16].

The East-West [19] effect

In Ref. [19] the east-west effect was seen in neutrinos for the first time. This effect, first since in cosmic ray showers, is a direct confirmation of the mostly positively charged nature of the cosmic rays. Low-energy cosmic rays are deflected by the Earth's magnetic field distorting the measured azimuthal spectra. By selecting a subset of events sensitive to the Earth's magnetic field this effect was observed as shown in Fig. 4 taken from [19].

While the previous analyses explored only zenith angle distortions caused by oscillations, by confirming the expected azimuthal distortion it was demonstrated that the geomagnetic effects on the production of GeV energy neutrinos was well understood.

Tests for non-standard oscillation models [20]

As more data was collected and the techniques were improved much effort was put into trying to test if any other explanation was as good as the $\nu_\mu \leftrightarrow \nu_\tau$ at explaining the observed data.

In Ref. [20] with over 1000 days of data the fully and partially contained events were fit together along with the upward-going muons and a multi-ring sample which had been enriched with neutral-current interactions. In $\nu_\mu \leftrightarrow \nu_\tau$ oscillations, a simple disappearance of the charged current events would be expected since tau

neutrinos still have neutral current interactions. On the other-hand, if the oscillations were to sterile neutrinos which had no interactions at all, two additional effects would arise. First, there would also be a reduction in the neutral current sample. Second, because of a difference in the forward scattering cross-sections in the two cases, the normal charge current oscillations would be suppressed at high energies. This suppression is known as the “matter effect.” A fit was done to the data samples looking for these effects and was not seen. Instead, the data fit the standard $\nu_\mu \leftrightarrow \nu_\tau$ hypothesis extremely well and excluded oscillations into sterile neutrinos at greater than the 99% hypothesis level.

Observation of the oscillation pattern [21]

In 2004 in Ref. [21] the standard oscillation hypothesis was given strong confirmation by the observation of a sinusoidal pattern in the oscillation pattern.

Since the oscillation equation contains a sin function, in principle one should be able to see a sinusoidal dip if the data is plotted as a function of L/E . However, in the standard analyses, low resolution in reconstructed L (distance from production) and E (neutrino energy) washes out the effect if the data is plotted in these combinations of variables. In Ref. [21] a subset of events were selected which had high resolution in these variables and after plotting the observed suppression relative to the expectation as a function of L/E the tell-tale dip from oscillations was observed. Additionally, by

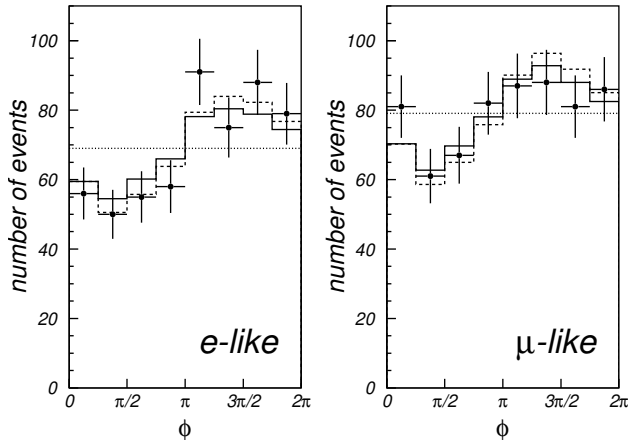


FIG. 4: Azimuthal angle distributions of e -like and μ -like events. The crosses represent the data points, the histogram drawn by solid line (dashed-line) shows the prediction of the Monte Carlo based on the flux of [two different flux models]. Data are shown with statistical errors. The Monte Carlo has 10 times more statistic than data. The Monte Carlo histogram is normalized to the total number of the real data. ϕ represents the azimuthal angle. $\phi = 0, \pi/2, \pi$ and $3\pi/2$ shows particles going to north, west, south, and east, respectively. Figure and caption from Ref. [19].

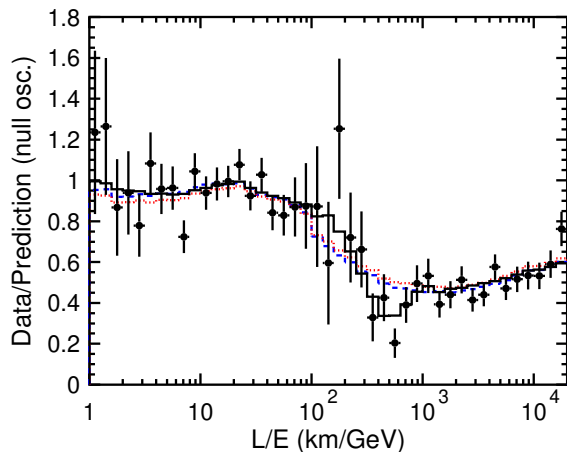


FIG. 5: Ratio of the data to the MC events without neutrino oscillation (points) as a function of the reconstructed L/E together with the best-fit expectation for 2-flavor $\nu_\mu \leftrightarrow \nu_\tau$ oscillations (solid line). The error bars are statistical only. Also shown are the best-fit expectation for neutrino decay (dashed line) and neutrino decoherence (dotted line). Figure and caption from Ref. [21]

comparing the χ^2 of the data to the standard oscillation scenario to that of neutrino decay and decoherence those other exotic hypothesis could be rejected with high

significance. Figure 5 demonstrating the effect is taken from Ref. [21].

Measurement of atmospheric neutrino parameters [12]

In 2005 all of the data from SK-I was refitted. This time the fit was done jointly with all of the data including upward-going and multiple ring-samples together. Ref. [12] describes this analysis in detail along with details of the atmospheric neutrino Monte Carlo and reconstruction algorithms and reduction.

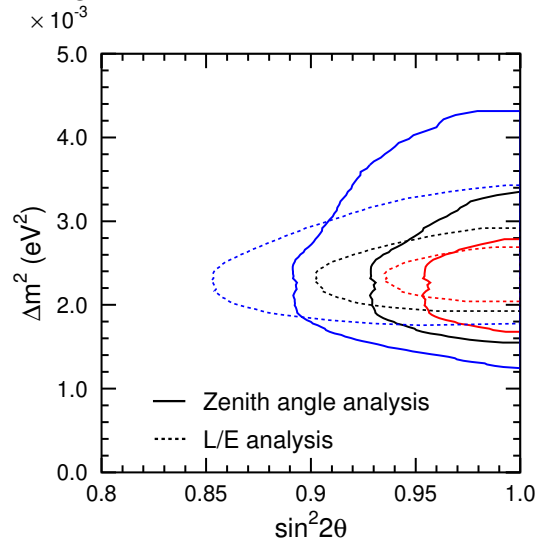


FIG. 6: The 68, 90 and 99% confidence level allowed oscillation parameter regions obtained by an L/E analysis [21] and by the 2005 complete data-set analysis are compared. Note the use of the linear y-scale in the figure. Figure from Ref [12].

Thirty-nine systematic uncertainties were accounted for in the fit, and the best fit for $\nu_\mu \leftrightarrow \nu_\tau$ oscillations with $\sin^2 2\theta = 1.00$ and $\Delta m^2 = 2.1 \times 10^{-3} \text{ eV}^2$ was found. Figure 7, taken from Ref. [12] and shown on the next page, displays all of the data samples and the results of the fit. Over 15,000 atmospheric neutrino events were used in the analysis. In Fig. 6 the final allowed region is shown along with the allowed region that is found by the L/E analysis from Ref. [20]. Both of these analyses give consistent results. The better constraint in $\sin^2 2\theta$ in the zenith angle analysis is due to higher statistics in the sample, while the better constraint in Δm^2 in the L/E analysis is due to finer binning in the fit. Later, as yet unpublished analyses combine the best feature of both techniques to extract the maximum information.

Three flavor oscillations [22]

In Ref. [12] the data was fit assuming that there were only oscillations between two flavors of neutrinos. How-

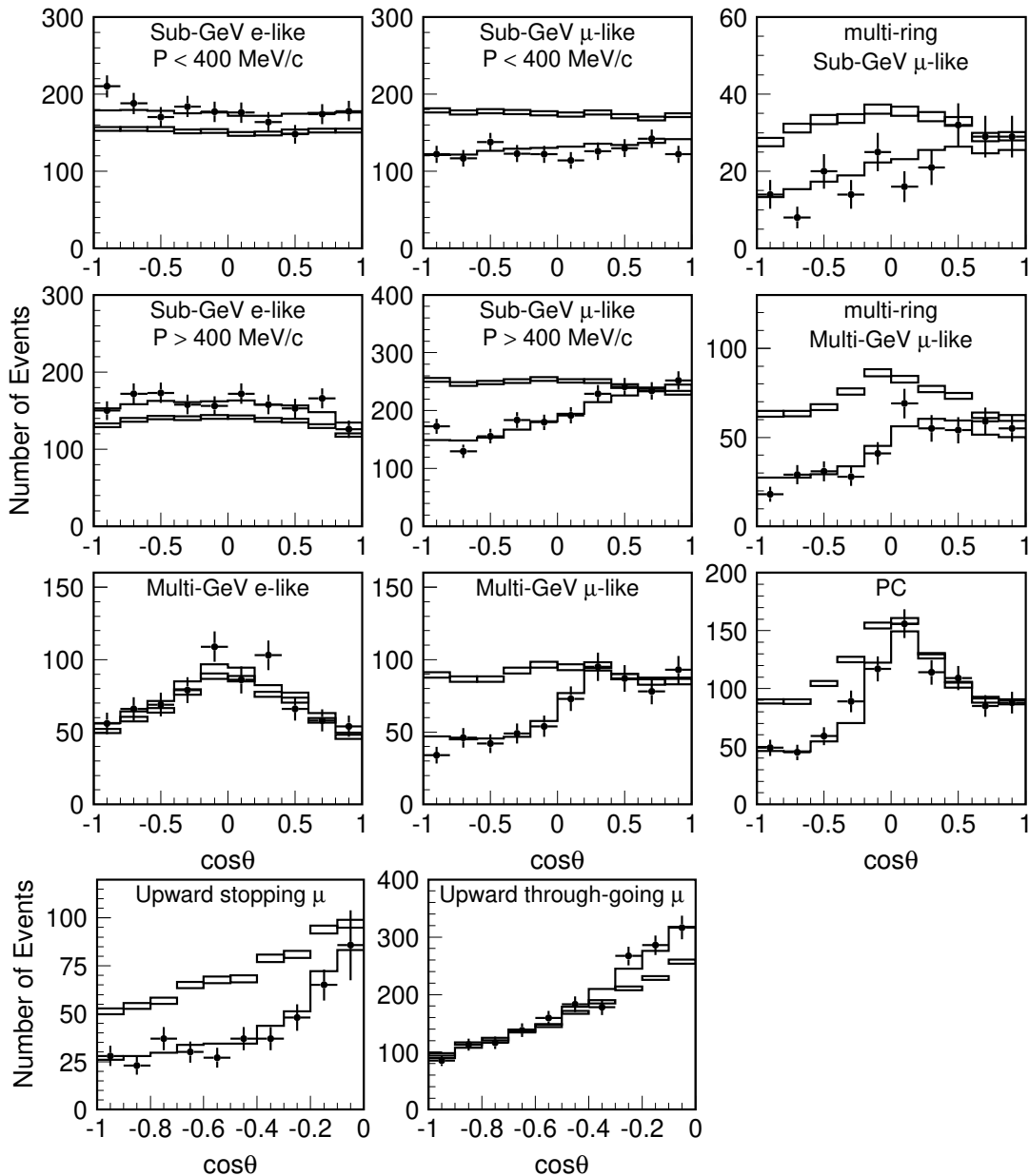


FIG. 7: The zenith angle distribution for fully-contained 1-ring events, multi-ring events, partially-contained events and upward muons. The points show the data, box histograms show the non-oscillated Monte Carlo events and the lines show the best-fit expectations for $\nu_\mu \leftrightarrow \nu_\tau$ oscillations with $\sin^2 2\theta = 1.00$ and $\Delta m^2 = 2.1 \times 10^{-3} \text{ eV}^2$. The best-fit expectation is corrected by the 39 systematic error terms, while the correction is not made for the non-oscillated Monte Carlo events. The height of the boxes shows the statistical error of the Monte Carlo. Figure and caption from Ref. [12].

ever, we know there are three flavors of neutrinos and one can write down a three-flavor mixing matrix with three mixing angles. The two that have been measured (θ_{12} and θ_{23}) control solar and atmospheric mixing respectively. The third, as yet unmeasured, mixing angle θ_{13} would allow all three of these neutrinos to oscillate into each-other, producing small amounts of high energy electron neutrino appearance in the upward going data. The question of the value of θ_{13} is particularly pressing since if it is extremely small or zero it will not be possible

to measure CP violation in the neutrino sector using the oscillation technique.

In order to measure or constrain the value of θ_{13} using the Super-K data set, a fit was performed using full three flavor oscillation probabilities, taking into account the resonance effects that can occur in the earth for such oscillations. The data was binned so as to be maximally sensitive to upward going electrons in the relevant energy regions. As detailed in Ref. [22] no evidence for non-zero θ_{13} was found. A plot showing the

Super-K θ_{13} allowed region overlaid with the exclusion region for the CHOOZ reactor experiment is shown in Fig. 8.

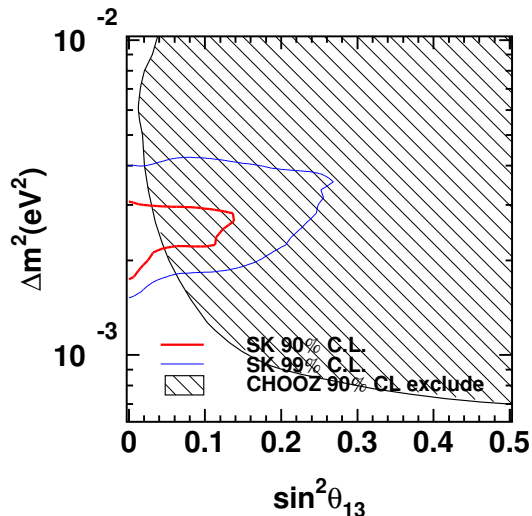


FIG. 8: Allowed regions of θ_{13} as found in the SK-I data set in the three flavor oscillation analysis. 90 % (thick line) and 99 % (thin line) confidence level allowed regions are shown in Δm^2 vs $\sin^2 \theta_{13}$. Normal mass hierarchy ($\Delta m^2 > 0$) is assumed. The shaded area in the bottom figure shows the region excluded by the CHOOZ reactor neutrino experiment. From Ref [22].

Search for tau lepton appearance [23]

None of the previous analyses explicitly searched for the appearance of the tau lepton from oscillations. The number of tau leptons in the data sample is expected to be small. Only on the order of 80 events with tau leptons were expected to be produced in fiducial volume of Super-Kamiokande during the SK-I running period. In Ref. [23] an explicit search for tau lepton appearance was undertaken.

This search relied on the fact that events containing heavy tau leptons which decay hadronically, decay symmetrically with more pions in the final state than the charged current deep-inelastic events which form the background to the search. A statistical separation of signal to background was made using both a likelihood and a neural-network. The background was normalized with downward going events by taking advantage of the fact that the entire tau signal comes from below. Fig 9 from Ref. [23] shows the results of the fit. This analysis measured a tau appearance signal which was consistent with that expected from $\nu_\mu \leftrightarrow \nu_\tau$ oscillations.

B. Solar Neutrino Oscillations

The neutrinos produced in the nuclear burning of the sun are of lower energy than atmospheric neutrinos.

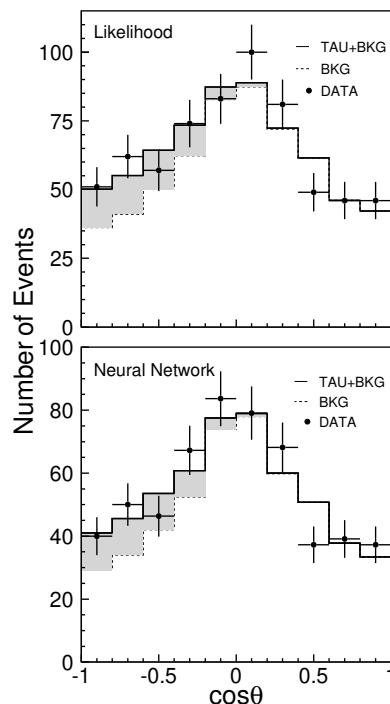


FIG. 9: The zenith angle distributions for the likelihood (top) and neural network (bottom) analyses. Zenith angle $\cos\theta = -1$ ($\cos\theta = +1$) indicates upward-going (downward-going). The data sample is fitted after tau neutrino event selection criteria are applied. The solid histogram shows the best fit including ν_τ , and the dashed histogram shows the backgrounds from atmospheric neutrinos (ν_e and ν_μ). An excess of tau-like events is observed in upward-going direction (shaded area). From Ref. [23]

Super-Kamiokande is sensitive mostly to neutrinos from the 8B branch of the pp nuclear fusion chain in solar burning. At very low energies the experiment is dominated by radioactive backgrounds. However, above approximately 4 MeV the detector can pick-out the scattering of solar neutrinos off atomic electrons which make Cherenkov light in the tank. The 8B and rarer HEP neutrinos have a spectrum which ends near 20 MeV.

Unlike previous radio-chemical experiments which relied on extraction of isotopes, Super-Kamiokande collects its data in real time and the electrons which are scattered by neutrinos point in a direction that is correlated with the sun. Therefore, by plotting the direction between low energy events in the tank and the Sun, one can pick out a peak containing solar neutrinos. This is clearly demonstrated in Fig. 10 which the cos of the angle between the events and the sun are plotted.

The first solar neutrino results from Super-Kamiokande were presented in 1998 in Ref. [24] and reported the measured flux from the first 300 days of data. In this paper, only the measured rate was reported and Super-Kamiokande confirmed the existence

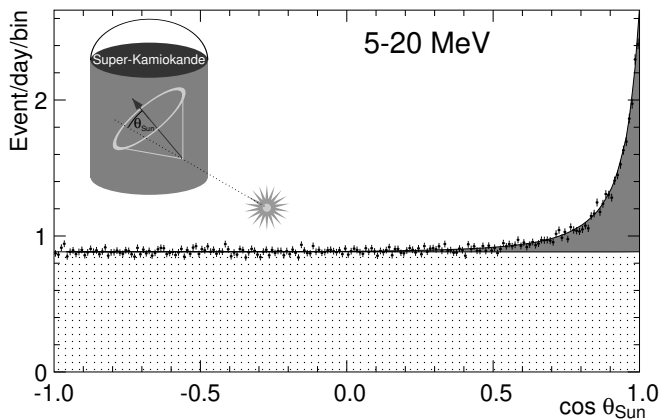


FIG. 10: Angular distribution of solar neutrino event candidates. The shaded area indicates the elastic scattering peak. The dotted area is the contribution from background events. From Ref. [13]

of deficit in neutrinos expected from by the sun. It was consistent with the previous Kamiokande measurement and reported a flux which was 36% of the standard solar model of 1995. For this first analysis, the energy threshold was set at 6.5 MeV which was later lowered.

The next two papers used 504 days of data and searched for distinctive signs of neutrino oscillation. In Ref [25], a measurement was made of the solar flux as measured at Super-Kamiokande in the day and the night separately. During the day, neutrinos from the sun travel down from above, traveling through very little earth. While during the night they travel from the other side of the Earth, in some parts of the year actually passing through the outer core. This is relevant because, for some regions of oscillation space, a regeneration of the original flux can happen inside high density materials. In this paper, no statistically significant sign of this was seen, thereby excluding parts of the oscillation space previously allowed by other experiments. At the same time, an analysis of the measured energy spectrum shape was published in Ref. [26] using the 504 day data set. It was found that a χ^2 analysis gave a a probability of 4.6% of being in agreement with the standard solar model.

In 2001, with more than twice as much data, the analysis threshold was lowered to 5 MeV and the systematics of the measurement were reduced due to extensive calibrations and improvements in the analysis techniques. In Ref. [27] a precise measurement of the solar flux was found. Additionally, the spectrum was found to have no significant energy spectrum distortions, and a no statistically significant day-night effect was seen. The small but expected seasonal variation of the flux due to the eccentricity of the Earth's orbit was observed and new stringent limits on the flux of HEP neutrinos were presented. The lack of spectral and zenith angle distortions placed strong constraints on the oscillation solutions to the solar neutrino problem and in Ref. [28] an oscilla-

tion analysis was performed using both the spectral and flux information from Super-Kamiokande. The result of this analysis was a preference for the Large Mixing Angle solution.

In 2002 an analysis including all 1496 days of SK-I was published [29]. The lack of spectral distortion and daily variation in the flux strongly constrained the regions allowed for neutrino oscillation from other experiments, leaving only the high-mass LMA and quasi-vacuum region allowed. If the Super-K interaction rate and either the standard solar model prediction of the 8B flux, or the rates as measured by SNO were included in the analysis, the LMA angle was uniquely allowed at high confidence level. This single allowed region could uniquely explain the solar neutrino problem.

The full SK-I data set was also used to search for other exotic signals from the Sun. First was the search for anti-electron neutrinos in Ref. [30]. The motivation for this search was to exclude the possibility that the electron-neutrinos from the sun are disappearing do to a spin-flavor-precession where neutrinos with a large magnetic moment are transformed into their anti-particles in the strong magnetic field of the sun. Unlike the standard solar neutrino analysis, the reaction here is inverse beta-decay off of protons in the nucleus. No signal was found and a limit was set of 0.8% of the standard solar neutrino flux between 8-20 MeV.

Next, in Ref. [31], searches for periodicity in the solar neutrino data using the Lomb test were performed. No significant statistical fluctuation was found. Finally, in 2004, a search for the magnetic moment of the neutrino was presented in Ref. [32]. The SK-I data set was used to look for energy distortion of electron recoil spectrum. Using Super-Kamiokande's allowed oscillation parameters a limit of $< 3.6 \times 10^{-10} \mu_B$ was set. If the constraints on oscillation parameters from other experiments were also included then the limit was reduced to $< 1.1 \times 10^{-10} \mu_B$.

In 2004, in Ref. [33], the full SK-I data set was once again analyzed but this time with a maximum likelihood analysis applied to the zenith angle dependence of the data. This lowered the statistical uncertainty on the day/night ratio by 25% compared to the previous measurement. This was equivalent to adding three years of live-time running if still using the previous method. Fig. 11 from Ref. [33] shows the data and best fit spectrum in the LMA region along with the D/N asymmetry as a function of energy.

In 2005 a full detailed description of the SK-I solar neutrino analysis was published in Ref. [13]. This paper included descriptions of the simulation, reconstruction and analysis techniques. In the large mixing angle region the day-night asymmetry was found to be:

$$A = \frac{(\Phi_D - \Phi_N)}{\frac{1}{2}(\Phi_D + \Phi_N)} = -1.7\% \pm 1.6\%(stat.)_{-1.2\%}^{+1.3\%}(sys.) \pm .04\%(\Delta m^2) \quad (5)$$

which is statistically compatible with zero and is to be

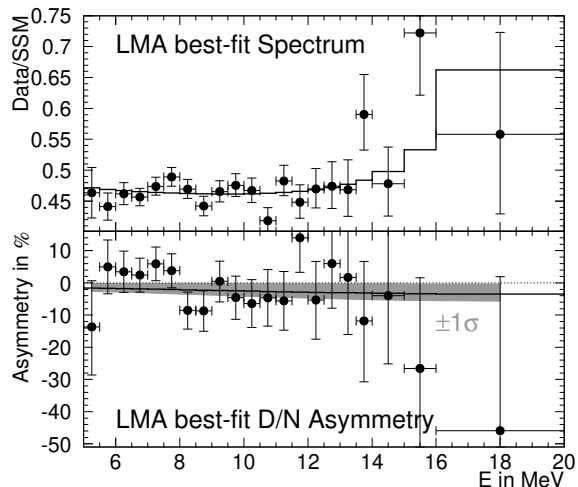


FIG. 11: LMA Spectrum (top) and D/N Asymmetry (bottom). The predictions (solid lines) are for $\tan^2 \theta = 0.55$ and $\Delta m^2 = 6.3 \times 10^{-5} \text{eV}^2$ with $\phi_{sB} = 0.96 \times \text{Standard Solar Model}$ [BP2000] and $\phi_{hep} = 3.6 \times \text{Standard Solar Model}$. Each energy bin is fit independently to the rate (top) and the day/night asymmetry (bottom). The gray bands are the $\pm 1\sigma$ ranges corresponding to the fitted value over the entire range 5-20 MeV: $A = -1.8 \pm 1.6\%$. Figure and caption from Ref. [33].

compared with the expected asymmetry which ranges from -1.7% to 1.0%.

C. The Search for Proton Decay

Super-K has also set important limits on the decay of the nucleon. The limits from Super-K have ruled out SU(5) and the minimal super-symmetric model. The published limits on $p \rightarrow e^+ \pi^0$ as predicted in SU(5) are found in Ref. [34].

Many models of super-symmetry predict that the nucleon should decay with strange quarks in the final state. The first 535 days of SK data were analyzed to search for $p \rightarrow \bar{\nu} K^+$ and the limits were presented in Ref. [35]. In 2005 the full SK-I data set was employed to search for SUSY mediated decays of the proton. In the analysis presented in Ref. [36] stringent limits were set on $p \rightarrow \bar{\nu} K^+$, $n \rightarrow \bar{\nu} K^0$, $p \rightarrow \mu^+ K^0$ and $p \rightarrow e^+ K^0$ modes.

A related search for SUSY generated physics is the search for neutral Q-Balls as presented in Ref. [37]. Q-balls are topological solitons predicted in some SUSY models and interact as they pass through the Super-K tank leaving a trail of pions in their wake. A search was carried out using 542 days of the SK-II data set. No evidence for Q-balls were found, and Super-K finds the lowest limits in the world for Q-ball cross-sections below 200 mb.

D. The Search for Astrophysical Phenomenon

Super-Kamiokande has been used to search for several sources of neutrinos from outside of our solar system. Gamma Ray Bursters are among the most luminous sources that have ever been observed in the universe. Super-K performed a search for neutrinos that were in coincidence with the BATSE detector located on NASA's Compton Gamma Ray Observatory. The entire Super-K data sample from 7 MeV to ~ 100 TeV was compared with the BATSE online catalog in the period of April 1996 to May of 2000. The results were presented in Ref. [38] and no statistically significant signal was found.

A supernova which occurred in the center of our galaxy would produce on the order of 10,000 interactions inside the Super-Kamiokande tank, yielding a rich sample of events for analysis. In the period of Super-K running there has been no observed galactic supernova. In Ref. [39] a limit on the rate of core-collapse supernovae out to 100 kiloparsecs using the SK-I and SK-II data sets was reported to be $< 0.32/\text{year}$. Although no core collapse was detected by Super-Kamiokande, it is believed that the universe should be bathed in the relic neutrinos of all of the supernovas that have exploded in the past. In Ref. [40] the SK-I data sample was examined for such events. There is a region of energy between the endpoint of solar the solar neutrino spectrum and before the decay electrons of cosmic ray muons where one can hope to see the small number of expected events. No excess over background was observed, setting a limit just above the expected signal from many models.

The upward-going muons used for the atmospheric oscillation analysis can also be used to search for high energy sources of neutrinos. The only muons that come from below the tank are generated by neutrinos, and the neutrinos that produce them range from approximately 100 GeV to 100 TeV.

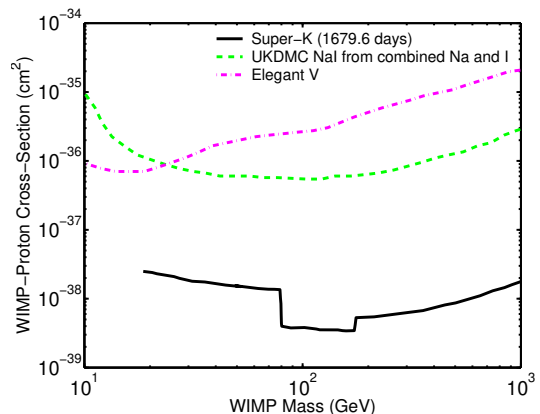


FIG. 12: Super-K 90 % CL exclusion region in WIMP parameter space for a WIMP with spin-dependent coupling along with corresponding 90 % CL exclusion limits from UKDMC (dashed) and ELEGANT (dot-dashed). Figure and caption from Ref. [41].

In addition to looking for neutrinos from astrophysical objects there is an expected neutrino signal from WIMP dark matter. Since WIMPs undergo gravitational attraction they are expected to gravitate around heavy bodies such as the Earth and the Sun. If a WIMP and anti-WIMP annihilate near the center of one of these objects where they have accumulated, they will decay into standard model particles some of which decay into neutrinos.

Therefore, if there is an excess signal of upward going neutrinos coming from either the center of the Earth or the Sun it can be interpreted as a signal for dark matter. It is shown in Ref. [41] that the limit on spin-dependent couplings inferred from the lack of an excess in the direction of the sun is on the order of 100 times more sensitive than comparable terrestrial direct dark matter experiments. Fig. 12 taken from Ref. [41] shows a comparison with the Super-K limits with that of other direct-detection experiments.

Additionally, several pure astronomical analyses have been performed with Super-K using samples of both downward-going and upward-going muons. In Ref. [42] the anisotropy of the primary cosmic ray flux with a mean energy of 10 TeV was measured by studying the relative sidereal variation of downward-going muons in the Super-K tank.

By using upward-going muons, searches were performed for sources of high energy astrophysical neutrinos. In Ref. [43] the sample of upward-going muons were used to search the sky for point sources and signatures of a diffuse flux of neutrinos from the galactic plane. Additional time correlated searches with some known sources were also performed. Above 1 TeV of muon energy, the flux of upward going muons from atmospheric neutrinos becomes small enough to look for a diffuse flux of extremely high energy neutrinos from astrophysical sources such as active galactic nuclei. In Ref. [44] the outer detector of Super-K was used to measure the direction of extremely high energy events. One event was found which was consistent with the background expectation and limits were set on this flux.

IV. CONCLUSIONS

This review of the published work of the Super-Kamiokande collaboration has shown the depth and importance of the work that the experiment has achieved. From astronomy and astrophysics, to tests of grand unified models, and to the observation of neutrino mass using neutrinos from the atmosphere and the Sun, Super-K has had a major impact on particle physics.

It would be a mistake to take this snapshot of the published work of Super-Kamiokande as its final word. There is a large data set from SK-II which is currently being analyzed, and will soon be published. These analyses will increase the precision of the parameters Super-Kamiokande has already measured. In addition, the larger data set will allow analyses for more subtle effects

which have not yet been studied.

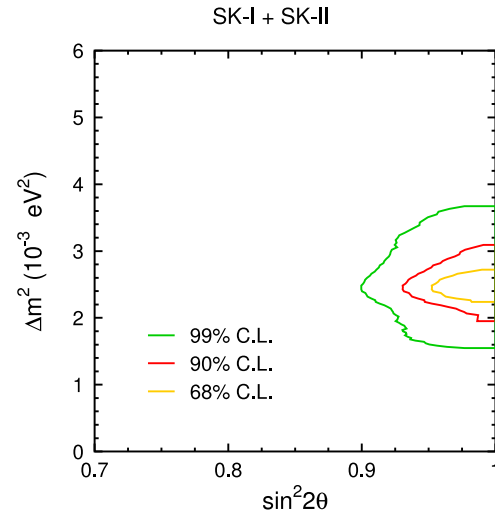


FIG. 13: Preliminary allowed region of atmospheric oscillation parameters using the combined data sets of SK-I and SK-II. The fit to the data employed 380 bins, 70 systematic errors and had a Chi-squared probability of 18%. Note the use of the linear y-scale in the figure.

As one example of this, Fig. 13 shows the latest result of the atmospheric oscillation analysis using the combined SK-I and SK-II data sets. In addition to the increase in statistics this analysis has improvements in the binning and systematic errors. It should be noted that in this figure the y-axis is plotted on a linear scale.

This analysis employed 380 bins and 70 systematic errors. The best fit to the atmospheric oscillation parameters were:

$$\Delta m^2 = 2.5 \times 10^{-3} eV^2 \quad \sin^2 2\theta = 1.00, \quad (6)$$

with the allowed region at 90% CL being equal to:

$$1.9 \times 10^{-3} eV^2 < \Delta m^2 < 3.1 \times 10^{-3} eV^2 \quad \sin^2 2\theta < 0.93. \quad (7)$$

Since June of 2006 SK-III has been operational and taking data. Fig 14 is a picture of SK-III during filling before operations commenced. Super-Kamiokande will continue to collect data, wait for supernovae, and in 2009 will once again become a target for an accelerator based neutrino beam.

Acknowledgments

The author and the Super-Kamiokande collaboration gratefully acknowledge the cooperation of the Kamioka Mining and Smelting Company. The Super-Kamiokande experiment has been built and operated from funding by the Japanese Ministry of Education, Culture, Sports, Science and Technology, the United States Department of Energy, and the U.S. National Science Foundation.

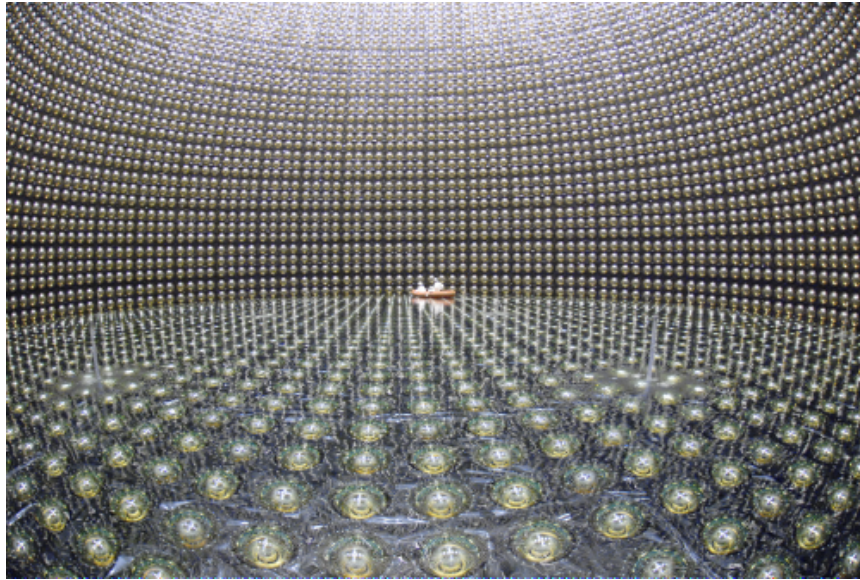


FIG. 14: Picture of SK-III during filling and before the beginning of operations. *Photo-credit: Kamioka Observatory, ICRR(Institute for Cosmic Ray Research), The University of Tokyo.*

-
- [1] K. S. Hirata et al. (KAMIOKANDE-II), Phys. Lett. **B205**, 416 (1988).
- [2] K. S. Hirata et al. (Kamiokande-II), Phys. Lett. **B280**, 146 (1992).
- [3] D. Casper et al., Phys. Rev. Lett. **66**, 2561 (1991).
- [4] R. Becker-Szendy et al., Phys. Rev. **D46**, 3720 (1992).
- [5] H. Georgi and S. L. Glashow, Phys. Rev. Lett. **32**, 438 (1974).
- [6] M. Aglietta et al. (The NUSEX), Europhys. Lett. **8**, 611 (1989).
- [7] K. Daum et al. (Frejus.), Z. Phys. **C66**, 417 (1995).
- [8] Y. Fukuda et al., Nucl. Instrum. Meth. **A501**, 418 (2003).
- [9] M. Nakahata et al. (Super-Kamiokande), Nucl. Instrum. Meth. **A421**, 113 (1999), hep-ex/9807027.
- [10] E. Blaufuss et al. (Super-Kamiokande), Nucl. Instrum. Meth. **A458**, 638 (2001), hep-ex/0005014.
- [11] Y. Takeuchi et al. (SuperKamiokade), Phys. Lett. **B452**, 418 (1999), hep-ex/9903006.
- [12] Y. Ashie et al. (Super-Kamiokande), Phys. Rev. **D71**, 112005 (2005), hep-ex/0501064.
- [13] J. Hosaka et al. (Super-Kamkiokande), Phys. Rev. **D73**, 112001 (2006), hep-ex/0508053.
- [14] Y. Fukuda et al. (Super-Kamiokande), Phys. Lett. **B433**, 9 (1998), hep-ex/9803006.
- [15] Y. Fukuda et al. (Super-Kamiokande), Phys. Lett. **B436**, 33 (1998), hep-ex/9805006.
- [16] Y. Fukuda et al. (Super-Kamiokande), Phys. Rev. Lett. **81**, 1562 (1998), hep-ex/9807003.
- [17] Y. Fukuda et al. (Super-Kamiokande), Phys. Rev. Lett. **82**, 2644 (1999), hep-ex/9812014.
- [18] Y. Fukuda et al. (Super-Kamiokande), Phys. Lett. **B467**, 185 (1999), hep-ex/9908049.
- [19] T. Futagami et al. (Super-Kamiokande), Phys. Rev. Lett. **82**, 5194 (1999), astro-ph/9901139.
- [20] S. Fukuda et al. (Super-Kamiokande), Phys. Rev. Lett. **85**, 3999 (2000), hep-ex/0009001.
- [21] Y. Ashie et al. (Super-Kamiokande), Phys. Rev. Lett. **93**, 101801 (2004), hep-ex/0404034.
- [22] J. Hosaka et al. (Super-Kamiokande), Phys. Rev. **D74**, 032002 (2006), hep-ex/0604011.
- [23] K. Abe et al. (Super-Kamiokande), Phys. Rev. Lett. **97**, 171801 (2006), hep-ex/0607059.
- [24] Y. Fukuda et al. (Super-Kamiokande), Phys. Rev. Lett. **81**, 1158 (1998), hep-ex/9805021.
- [25] Y. Fukuda et al. (Super-Kamiokande), Phys. Rev. Lett. **82**, 1810 (1999), hep-ex/9812009.
- [26] Y. Fukuda et al. (Super-Kamiokande), Phys. Rev. Lett. **82**, 2430 (1999), hep-ex/9812011.
- [27] S. Fukuda et al. (Super-Kamiokande), Phys. Rev. Lett. **86**, 5656 (2001), hep-ex/0103033.
- [28] S. Fukuda et al. (Super-Kamiokande), Phys. Rev. Lett. **86**, 5651 (2001), hep-ex/0103032.
- [29] S. Fukuda et al. (Super-Kamiokande), Phys. Lett. **B539**, 179 (2002), hep-ex/0205075.
- [30] Y. Gando et al. (Super-Kamiokande), Phys. Rev. Lett. **90**, 171302 (2003), hep-ex/0212067.
- [31] J. Yoo et al. (Super-Kamiokande), Phys. Rev. **D68**, 092002 (2003), hep-ex/0307070.
- [32] D. W. Liu et al. (Super-Kamiokande), Phys. Rev. Lett. **93**, 021802 (2004), hep-ex/0402015.
- [33] M. B. Smy et al. (Super-Kamiokande), Phys. Rev. **D69**, 011104 (2004), hep-ex/0309011.
- [34] M. Shiozawa et al. (Super-Kamiokande), Phys. Rev. Lett. **81**, 3319 (1998), hep-ex/9806014.
- [35] Y. Hayato et al. (Super-Kamiokande), Phys. Rev. Lett. **83**, 1529 (1999), hep-ex/9904020.
- [36] K. Kobayashi et al. (Super-Kamiokande), Phys. Rev. **D72**, 052007 (2005), hep-ex/0502026.
- [37] Y. Takenaga et al. (Super-Kamiokande), Phys. Lett. **B647**, 18 (2007), hep-ex/0608057.

- [38] S. Fukuda et al. (Super-Kamiokande), *Astrophys. J.* **578**, 317 (2002), astro-ph/0205304.
- [39] M. Ikeda et al. (Super-Kamiokande), *Astrophys. J.* **669**, 519 (2007), arXiv:0706.2283 [astro-ph].
- [40] M. Malek et al. (Super-Kamiokande), *Phys. Rev. Lett.* **90**, 061101 (2003), hep-ex/0209028.
- [41] S. Desai et al. (Super-Kamiokande), *Phys. Rev.* **D70**, 083523 (2004), hep-ex/0404025.
- [42] G. Guillian et al. (Super-Kamiokande), *Phys. Rev.* **D75**, 062003 (2007), astro-ph/0508468.
- [43] K. Abe et al., *Astrophys. J.* **652**, 198 (2006), astro-ph/0606413.
- [44] M. E. C. Swanson et al. (Super-Kamiokande), *Astrophys. J.* **652**, 206 (2006), astro-ph/0606126.